JMEPEG (2008) 17:857–863
DOI: 10.1007/s11665-008-9245-1

1059-9495/$19.00

The Effect of the Ausforging-and-Tempering on the Microstructure and Mechanical Properties of Steel 86CrMoV7

Furen Xiao, Bo Liao, Guiying Qiao, and Shuzhe Guan

(Submitted September 1, 2007; in revised form April 4, 2008)

Thermomechanical treatment as an effective method has been carried out in order to obtain a better combination of high strength and excellent toughness. In this work, the hot deformation behavior of 86CrMoV7 steel has been studied, and then the process of ausforging has been designed. The microstructures and mechanical properties of 86CrMoV7 steel by (1) direct quenching after forging (ausforging) and tempering, (2) quenching-and-tempering and spheroidizing annealing have been investigated. The results show ausforging-and-tempering provides high strength but same toughness as classical quenching-and-tempering.

Keywords ausforging-and-tempering, mechanical properties, microstructure

1. Introduction

Shape-forming processes utilize effective methods associated with heat treatment procedures after hot deformation to refine microstructure and improve the mechanical properties (Ref 1, 2). Examples include forging bars, wire rods, and rolled plates of low-carbon and medium-carbon microalloyed steels (Ref 3-6). Scant research has been done on high-carbon alloyed steel for heavy forging. The steel 86CrMoV7 is used to manufacture heavy rolls weighing over 5 ton. For heavy forged parts, annealing after forging and quenching-and-tempering are important procedures for producing rolls. It is important to study the combined effect of forging with heat treatments in order to reduce heat treatment procedures. Hot deformation influences the martensitic transformation, martensite structure, and tempering processes (Ref 7). The dynamic and static recrystallization can occur during hot deformation and in intervals between the consecutive passes. By controlling the correct deformation parameter, the recrystallized austenite grains can be refined. The dynamically recrystallized grains with heterogeneous dynamic substructures can promote the martensitic phase transformation and increase the martensite start transformation temperature (Ref 8). This makes developing of the fine-grained austenite structure possible, and therefore development of the fine-grained transformation products of this phase, having a significant input into its strengthening and into the increase of its toughness.

Furen Xiao, Bo Liao, Guiying Qiao, and **Shuzhe Guan**, Key Laboratory of Metastable Materials Science and Technology, College of Materials Science and Engineering, Yanshan University, Qinhuangdao 066004, China. Contact e-mails: frxiao@ysu.edu.cn and cyddjyjs@263.net

In our previous work (Ref 9), as the hot deformation temperature was below the lowest temperature where recrystallization could occur in austenite, it had a great effect on the martensitic transformation of steel 86CrMoV7, with the results that the martensite transformation starting temperature (Ms) was increased and the martensitic microstructure after quenching was refined (Ref 9). Therefore, in order to achieve high mechanical properties by ausforging-and-tempering process for this steel, it is necessary to study dynamic and/or static recrystallization during the forging procedures to obtain fine prior austenite grains with work hardened microstructure. In this work, the hot deformation behavior of steel 86CrMoV7 was investigated to design the ausforging processes. Furthermore, the microstructures and mechanical properties of steel 86CrMoV7 after ausforging-and-tempering, quenching-and-tempering, and spheroidizing annealing were investigated. The aim is to discuss the possibility to reduce the heat treatment procedures for roll manufacture.

2. Experimental Procedure

The chemical composition of the steel 86CrMoV7 used in this investigation is listed in Table 1. The original material was produced in open-hearth furnace, then refined in vacuum refinery furnace, and cast into ingots of 60 mm diameter. The ingots were reheated to 1200 °C, held for 3 h, and forged into the bars about 16 mm diameter. The forged bars were cooled to room temperature in air. After forging, the forged bars were spheroidize annealed. During the spheroidizing annealing process, the specimens were heated to 800 °C, held for 2 h, and cooled to 720 °C, held for 3 h, then cooled to 250 °C in furnace, and finally cooled to room temperature in air.

The compression tests were carried out on the THEMECMASTOR-Z thermal simulator. The dimension of the hot compressive specimen was $\Phi 8 \times 10$ mm. The specimens were reheated to 1200 °C, then cooled to 750-1150 °C. In order to observe the microstructure after the dynamic recrystallization,

Table 1 Chemical composition of 86CrMoV7 steel, wt.%

C	Si	Mn	P	S	Cr	Ni	Mo	V
0.89	0.42	0.31	0.002	0.005	1.80	0.03	0.27	0.10

the 0.22-1.0 single compressive deformation with the strain rate of 0.1-10 s^{-1} was carried out immediately followed by cooling to room temperature in water. The specimen were held 10-90 s at same temperature after deformation, then cooled to room temperature in water in order to observe the microstructure after static recrystallization.

According to the microstructure resulting from dynamic and static recrystallization, the ausforging technology was designed. For ausforging-and-tempering experiments, the ingot was ausenitized at 1100 °C, and forged at temperatures ranging from 1000 to 800 °C, then quenched in oil directly. The rate of reduction was about 70%. After ausforging, the specimens were tempered at temperatures ranging from 600 to 790 °C for 5 h.

The microstructure and mechanical properties of the specimens with the classical quenching-and-tempering technology were also studied. By the classical quenching-and-tempering processes, the specimens after spheroidizing annealing were reheated to 820 °C for 2 h, and quenched in oil, then tempered at 700 °C for 5 h.

Lastly, the mechanical properties of the specimens after different heat treatments were measured. The size of tensile specimens is 10 mm gauge diameter and 100 mm gauge length. The microstructure of specimens was determined by using optical microscopy (OM) and transmission electron microscopy (TEM). For TEM observation, thin foils were prepared by a twin jet electropolisher in a solution containing 10% perchloric acid and 90% glacial acetic acid. The TEM examination was performed on H-800 TEM at 200 kV.

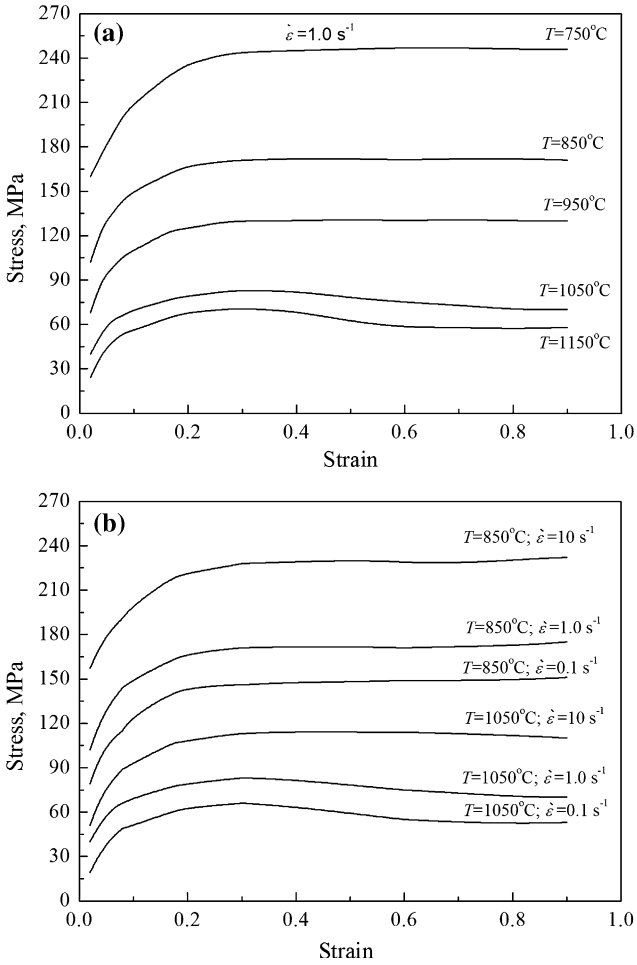

Fig. 1 Effect of the deformation temperature (a) and the strain rate (b) on the stress-strain curves of the tested steel

3. Results and Discussion

3.1 Hot Deformation Behavior

Typical stress-strain curves of this steel in the temperature range from 750 to 1150 °C and strain rate range from 0.1 to 10 s^{-1} are shown in Fig. 1. When the deformation temperature was higher than 1050 °C, and/or the strain rate was at 0.1 s^{-1}, a maximum characterized by peak strain (ε_p) and stress (σ_p) appeared in the curve, followed by a gradual fall to a constant stress (σ_{ss}) value. This is typical of materials for which dynamic recrystallization can be initiated dynamically when the specimen is deformed at temperature above half of their absolute melting point. With a decrease of the temperature or increase of the strain rate, the peak broadens and its stress and strain values are increased. As the deformation temperature decreases to 950 °C, and/or strain rate increases to 1.0 s^{-1}, the stress is increased with an increase of the strain, which is typical of work hardening. These results indicate that the lowest temperature where recrystallization will occur of this steel is lower than 950 °C. This needs to be confirmed by microstructural observation.

The typical microstructures of specimen cooled in water directly after deformation are shown in Fig. 2 and 3. When the deformation temperature is 1050 °C, some jagged grain boundaries can be observed at a strain of 0.22. Furthermore, some smaller dynamically recrystallized grains can be observed around some prior austenite grain boundaries (Fig. 2a). With increasing strain, the fraction of dynamic recrystallization increases (Fig. 2b). When the strain increases to 0.68, the fraction of dynamic recrystallization becomes almost 100% (Fig. 2c). Upon farther increasing the strain, dynamically recrystallized austenite grains change little and become more uniform (Fig. 2d). These results are in accord with the stress-strain curves.

When the deformation temperature is decreased to 950 °C, the dynamically recrystallized grains are not observed when strain is 0.22 (Fig. 3a). When strain increases to 0.68, the prior austenite grains become elongated, and some deformation bands and twin-crystals can be observed in prior austenite grains (Fig. 3b). Furthermore, some dynamically recrystallized grains can be observed around prior austenite grain boundaries (Fig. 3b). When the strain increases to 1.0, the fraction of dynamic recrystallization is only about 35% (Fig. 3c). With decreasing strain rate, the fraction of recrystallization and the size of dynamically recrystallized grains are increased (Fig. 3d). These results are a little different to that of the stress-strain curves, which is a typical one of the work hardening. Therefore, to study the dynamic recrystallization of steel, the stress-strain curves must be combined with the microstructure analysis. When deformation temperature is decreased to 850 °C, even at

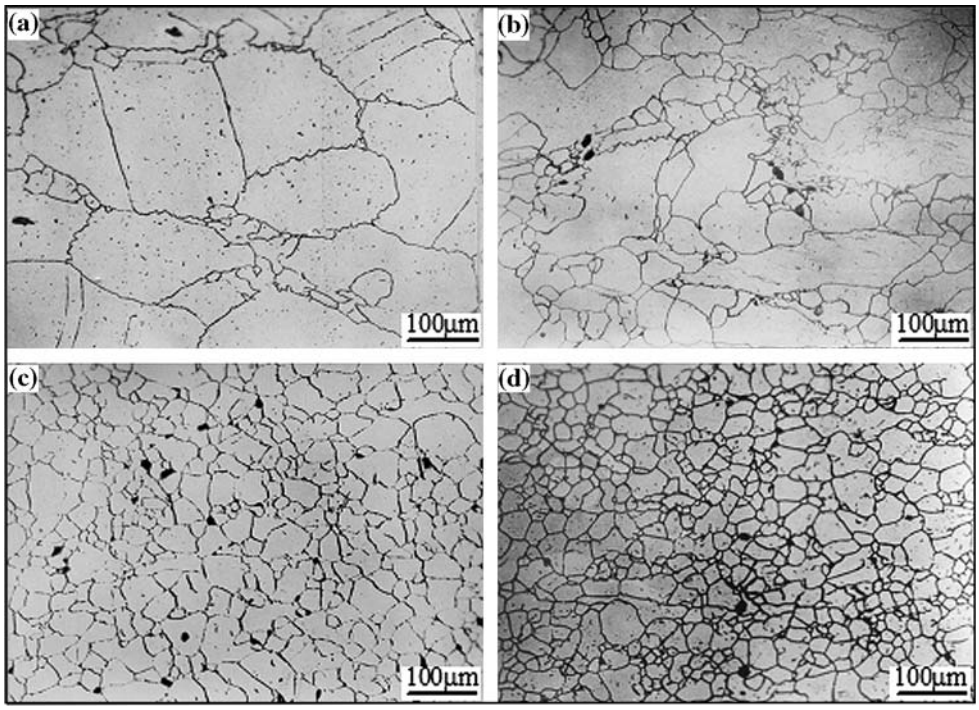

Fig. 2 Microstructural changes in specimens hot deformed at 1050 °C, strain rate of 1 s^{-1} and stain of (a) 0.22, (b) 0.42, (c) 0.68, and (d) 1.0

unit strain, the recrystallized grains cannot be observed on the specimen, and the microstructural characteristics represent massive deformation bands in the elongated prior austenite grains (Fig. 3e).

The effect of the static recrystallization on the deformed austenite microstructure is obvious. The typical microstructures of the specimen after deformation held from 10 to 90 s are shown in Fig. 4. When the specimen is deformed at 1050 °C, the static recrystallization completes quickly, and the austenite grain begins to grow, even if the holding time is very short (Fig. 4a, b and 2). When the deformation temperature is decreased to 950 °C, the time of total static recrystallization is prolonged (Fig. 4c and d). The 100% static recrystallization can be obtained in large deformation and long holding time (Fig. 4d). When the deformation temperature is decreased to 850 °C, the part of static recrystallization can be observed in the specimen after deformation and long holding time (Fig. 4e and f).

From the above results it is concluded that in order to obtain the prior austenite microstructure with refined austenite grain size and work hardening, the hot work technology parameters should be considered carefully.

3.2 Mechanical Properties of the Specimens After Different Heat Treatments

The mechanical properties of 86CrMoV7 steel after spheroidizing annealing, quenching-and-tempering, and ausforging-and-tempering are given in Table 2. The yield strength (σ_s) and tensile strength (σ_b) of the quench-and-tempered specimens are higher than those of the spheriodize annealed ones. In contrast, the elongation (δ_5) and reduction in area (ψ) of the quench-and-tempered specimens are a little lower than those of the spheriodize annealed ones. The quench-and-tempered specimens have higher strength and toughness. For ausforging-and-tempering, the tempering temperature has a great effect on mechanical properties. With increasing tempering temperature, the yield strength (σ_s) and tensile strength (σ_b) decrease, and the elongation (δ_5) and reduction in area (ψ) increase. When tempering temperature after ausforging is increased to 700 °C, the elongation (δ_5) and reduction in area (ψ) are similar to those of quench-and-tempered specimens; however, the yield strength (σ_s) and tensile strength (σ_b) are higher than those of the quench-and-tempered samples (80 MPa). The results indicate that ausforging-and-tempering is an effective method to improve the mechanical properties of metal materials. The mechanical properties after the ausforging-and-tempering at 790 °C are same as those after the spheroidizing annealing.

3.3 Microstructures of the Specimen After Different Heat Treatments

Typical optical micrographs of the specimen after different heat treatments are shown in Fig. 5. The microstructures of all samples are granular pearlite with granular carbides distributed in a ferrite matrix. Comparing the microstructures of the specimens after the spheroidizing annealing with those after quenching-and-tempering process, it is noted that the size of carbide particles in the quench-and-tempered specimens is smaller than that in the spheroidizing annealing specimens, and more uniformly distributed (Fig. 5a and b). For ausforging-and-tempering, as tempering temperature is lower than 650 °C, the fine precipitated carbide can be observed in the matrix (Fig. 5c). As tempering is higher than 700 °C, the microstructure is similar to that of quenching-and-tempering. With increasing tempering temperature, the size of carbide is increased (Fig. 5d-f).

The typical TEM micrographs of classical specimen are shown in Fig. 6. The microstructures of the specimens after different heat treatments consist of granular pearlite, which is

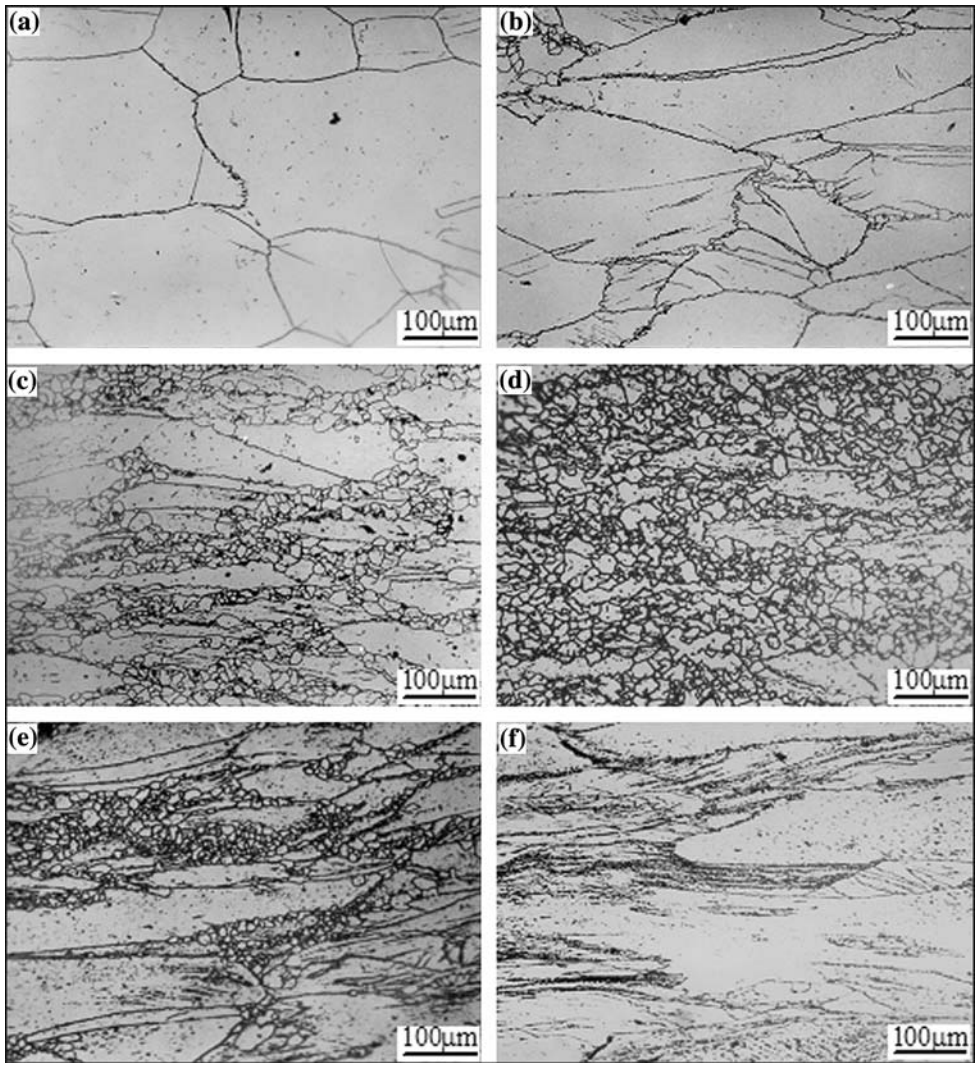

Fig. 3 Effect of deformation conditions on microstructure (a) $T = 950$ °C, $\dot{\varepsilon} = 1$ s^{-1}, $\varepsilon = 0.22$; (b) $T = 950$ °C, $\dot{\varepsilon} = 1$ s^{-1}, $\varepsilon = 0.68$; (c) $T = 950$ °C, $\dot{\varepsilon} = 1$ s^{-1}, $\varepsilon = 1.0$; (d) $T = 950$ °C, $\dot{\varepsilon} = 0.1$ s^{-1}, $\varepsilon = 1.0$; (e) $T = 950$ °C, $\dot{\varepsilon} = 1.0$ s^{-1}, $\varepsilon = 1.0$; and (f) $T = 850$ °C, $\dot{\varepsilon} = 0.1$ s^{-1}, $\varepsilon = 1.0$

ferrite matrix with granular carbides (Fig. 6a and b). However, the size of granular carbides in the specimens after quenching-and-tempering is smaller than the size in the annealed specimens (Fig. 6a and b). In addition, other different microstructural characteristics can be found in the TEM of both the specimens. In the spheroidize annealed specimens, the granular carbides are distributed in a ferrite matrix with lower dislocation density. The average size of granular carbides is about 2.4 μm (Fig. 6a). In the specimen after quenching-and-tempering, the size range of carbide is large and some sub-grain boundaries can be observed in the ferrite matrix. Furthermore, some refined carbide particles are distributed along sub-grain boundaries (Fig. 6b). The microstructure with refined carbide particles and sub-grain means that the quench-and-tempered specimens possess higher mechanical properties. In the case of ausforging-and-tempering, when the tempering temperature is 700 °C, the microstructure is similar to that of quenching-and-tempering (Fig. 6c). The sub-grains in specimen after ausforging-and-tempering are smaller than those in quench-and-tempered specimens, and the carbide particles are refined (Fig. 6b and c). Therefore, the mechanical properties of the ausforged-and-tempered specimens are higher than those of the quenching-and-tempering ones. When temperature is 790 °C, the microstructures of specimens are similar to those of the spheroidizing annealed specimen, while the carbides are smaller than those of the annealed specimen, and the dislocation density in matrix is higher than that of the annealed specimen, thereby resulting in higher mechanical properties.

As stated above, two typical microstructures can be found in the granular pearlite. One is that the granular carbides are distributed in ferrite matrix, in which no sub-grain can be found. Another is that the granular carbides are distributed at sub-grain boundary. For the first microstructure, according to the model of Ashby-Orowan, the effect of second phase particles on the strength is described by the following equation (Ref 10):

$$\sigma_p = \frac{10Gb}{5.72\pi^{3/2}r} f^{1/2} \ln\left(\frac{r}{b}\right) \quad \text{(Eq 1)}$$

where σ_p is the second phase strengthening, G the shear modulus, b the Burgers vector, r the mean planar intercept

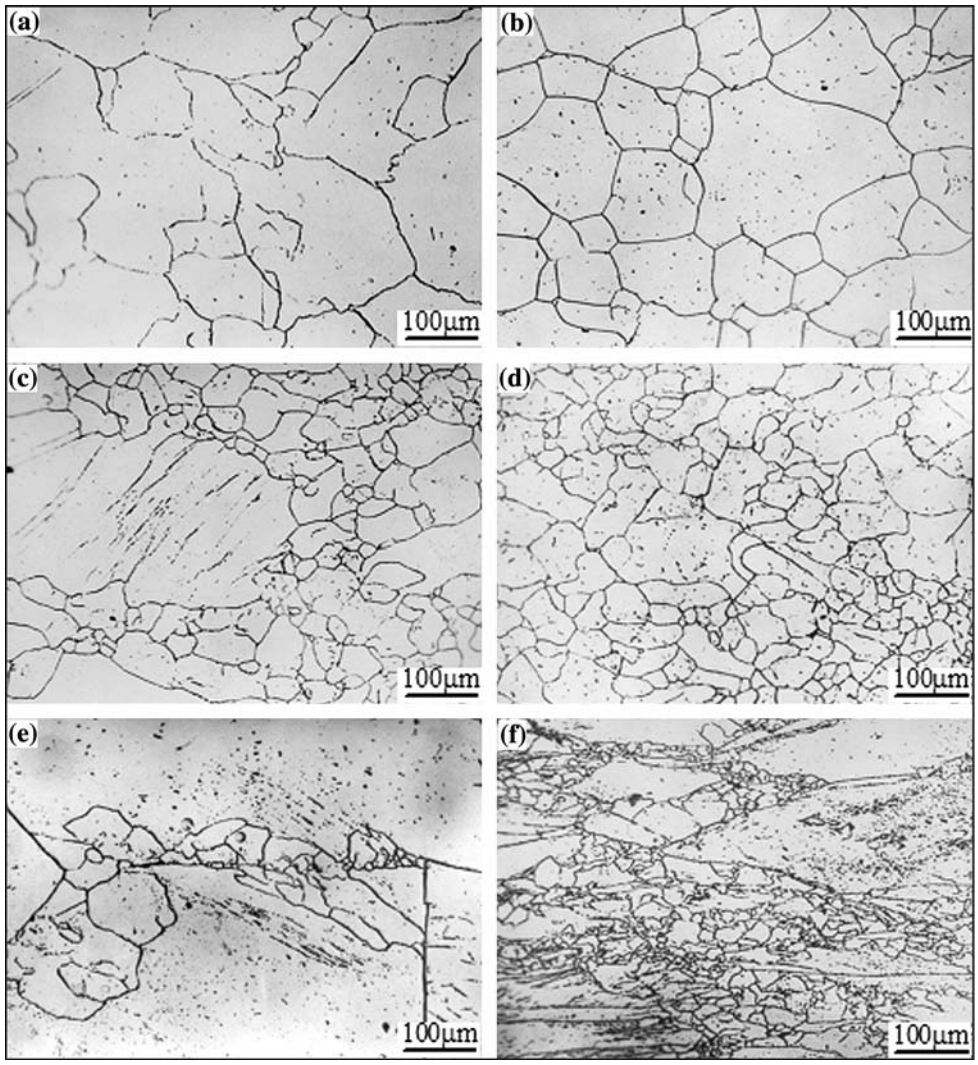

Fig. 4 Typical optical microstructure for different deformation conditions and holding time after deformation (a) $T = 1050$ °C, $\dot{\varepsilon} = 1$ s^{-1}, $\varepsilon = 0.22$, $t = 10$ s; (b) $T = 1050$ °C, $\dot{\varepsilon} = 1$ s^{-1}, $\varepsilon = 0.42$, $t = 10$ s; (c) $T = 950$ °C, $\dot{\varepsilon} = 1$ s^{-1}, $\varepsilon = 0.42$, $t = 10$ s; (d) $T = 950$ °C, $\dot{\varepsilon} = 1$ s^{-1}, $\varepsilon = 0.68$, $t = 10$ s; (e) $T = 850$ °C, $\dot{\varepsilon} = 1$ s^{-1}, $\varepsilon = 0.42$, $t = 90$ s; and (f) $T = 1050$ °C, $\dot{\varepsilon} = 1$ s^{-1}, $\varepsilon = 0.68$, $t = 90$ s

Table 2 The mechanical properties of the samples after different heat treatment processes

Process	Yield strength σ_s, MPa	Tensile strength σ_b, MPa	Elongation δ_5, %	Reduction in area ψ, %	HB
Spheroidizing annealing	423	712	26.3	60.5	189
Quenching-and-tempering	680	890	20.3	46.6	236
Ausforging and tempering at 600 °C	1284	1463	10.1	21.1	416
Ausforging and tempering at 650 °C	809	1163	13.3	25.5	323
Ausforging and tempering at 700 °C	770	973	19.4	46.8	268
Ausforging and tempering at 760 °C	434	761	25.1	57.0	199
Ausforging and tempering at 790 °C	428	760	26.8	62.7	195

diameter of the precipitates, and f the volume fraction of precipitation particles. Therefore, the strengthening effect of second phase for a material is related to the size of the second phase. As the size of the second phase particles is smaller, its effect on mechanical properties is stronger. In this case, the strength is determined by the grain size.

For the latter granular pearlite, in which the granular carbides are distributed at sub-grain boundaries, the strength can be expressed as follows (Ref 11):

$$\sigma_y = \sigma_i + k_y \lambda_{sg}^{-(1/2)} \quad \text{(Eq 2)}$$

where σ_y is the yield strength, σ_i is the lattice friction stress, k_y is constant, and λ_{sg} is the size of sub-grain. In this case, the effect of carbide particles is indirect. The strength is determined by the size of the sub-grain. Hence, the microstructure with refine sub-grain and fine carbide particles by ausforging-and-tempering process can effectively improve the mechanical properties of steels.

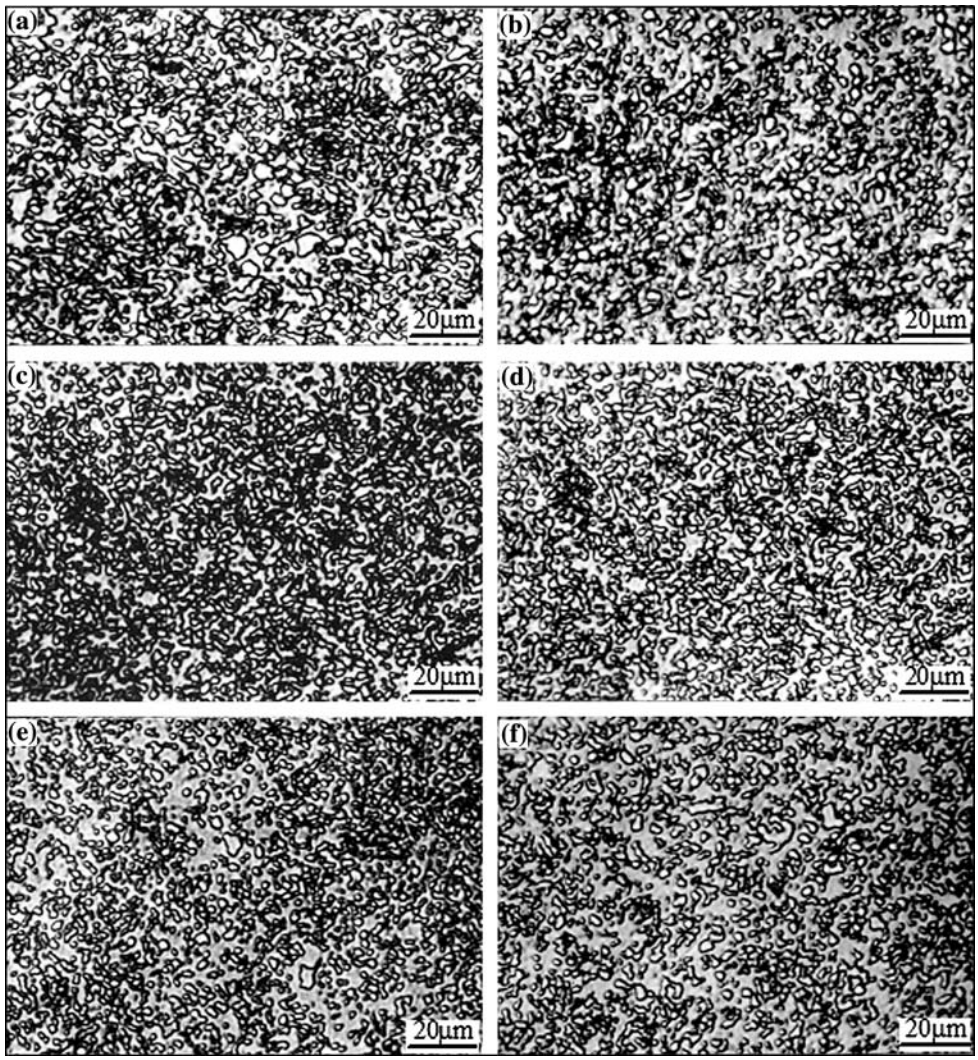

Fig. 5 Typical optical micrographs of samples after (a) spheridizing annealing, (b) quenching-and-tempering, and (c-f) ausforging-and-tempering at (c) 650 °C, (d) 700 °C, (e) 760 °C, and (f) 790 °C

The results of hot deformation research for 86CrMoV7 steel show that the recrystallization temperature is higher than 950 °C. As the deformation temperature is higher than 950 °C, the dynamic and/or static recrystallization occur during deformation, which results in the formation of fine prior austenite grains. If the temperature is decreased, it is beneficial to obtain the fine prior austenite grain (Fig. 1-4). When the hot deformation temperature is below 950 °C, recrystallization does not occur, which results in austenite work hardening (Fig. 1, 3, and 4). During hot deformation, the carbide is precipitated in substructure, which impedes the process of dynamic and static recrystallization. Therefore, during hot forging, especially at finishing forging temperature, a great deal of substructures, such as dislocation, sub-grain, and/or deformed bands appears in austenite matrix, and it is more stable due to carbide dynamic and/or static precipitation. The deformed austenite with high-density substructures remarkably affects martensitic microstructure after direct quenching. On one hand, it refines martensitic microstructure. On the other hand, some dislocations in deformed austenite can be inherited by martensite. The dislocation density in the hot deformed martensite is higher than that in martensite by the common quenching process. During tempering process, the precipitated carbides are finer and more dispersed than those in common quenched martensite, with the result that the substructures are finer and more stable. This is confirmed by comparing the microstructures after ausforging-and-tempering at 700 °C with those after quenching-and-tempering (Fig. 3b and c). Therefore, the specimens after ausforging-and-tempering have better combination of high strength and excellent toughness (Table 2). The control of the tempering temperature in ausforging process can provide considerable modification of the microstructure, and as a direct consequence, its mechanical properties are improved.

4. Conclusion

1. The mechanical properties of 86CrMoV7 steel can be improved by ausforging-and-tempering process designed by the results of the hot deformation behavior.
2. The prior austenite grains with extensive substructures are refined by controlling the forging process. Furthermore, the fine martensite microstructure with massive

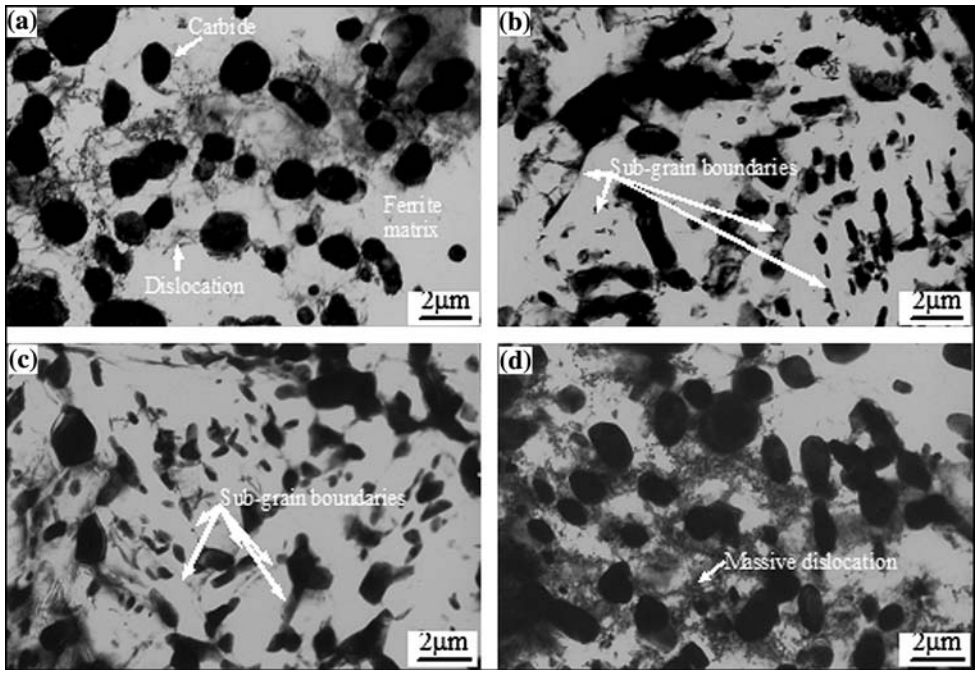

Fig. 6 TEM micrographs of samples after (a) spheridizing annealing, (b) quenching-and-tempering, (c) ausforging-and-tempering at 700 °C, and (d) ausforging-and-tempering at 790 °C

dislocations is obtained by ausforging. The tempering stability of the martensite can be improved. The carbides in granular pearlite after ausforging-and-tempering are finer and uniformly distributed, and the sub-grains are more stable. These resulting microstructures provide a high strength and excellent toughness to the steel. The control of the tempering temperature in ausforging-and-tempering process can provide considerable modification of the microstructure, and as a direct consequence, the mechanical properties of the steel can be improved.

References

1. I. Gonzalez-Baquet, R. Kaspar, J. Richter, G. Nussbaum, and A. Koethe, Influence of Microalloying on the Mechanical Properties of Medium Carbon Forging Steels After a Newly Designed Post Forging Treatment, *Steel Res.*, 1997, **68**, p 534–540
2. S.L. Zhang, X.J. Sun, and H. Dong, Effect of Deformation on the Evolution of Spheroidization for the Ultra High Carbon Steel, *Mater. Sci. Eng. A*, 2006, **432**, p 324–332
3. M. Jahazi and B. Eghbali, The Influence of Hot Forging Conditions on Microstructure and Mechanical Properties of Two Microalloyed Steels, *J. Mater. Process. Technol.*, 2001, **113**, p 594–598
4. J. Adamczyk and M. Opiela, Influence of the Thermo-Mechanical Treatment Parameters on the Inhomogeneity of the Austenite Structure and Mechanical Properties of the Cr–Mo Steel with Nb, Ti, and B Microadditions, *J. Mater. Process. Technol.*, 2004, **157–158**, p 456–461
5. T. Ochi, H. Takada, M. Kubota, H. Kanisawa, and K. Naito, Special Steel Bars and Wire Rods Contribute to Eliminate Manufacturing Processes of Mechanical Parts. Nippon Steel Technical Report 80, 1999, p 9–15
6. F. Xiao, B. Liao, Y.-Y. Shan, G.-Y. Qiao, Y. Zhong, C. Zhang, and K. Yang, Challenge of Mechanical Properties of an Acicular Ferrite Pipeline Steel, *Mater. Sci. Eng. A*, 2006, **431**, p 41–52
7. J. Huang and Z. Xu, Effect of Dynamically Recrystallized Austenite on the Martensite Start Temperature of Martensitic Transformation, *Mater. Sci. Eng. A*, 2006, **438–440**, p 254–257
8. L.M. Kaputkina and V.G. Prokoshkina, Martensitic Transformations and Martensite Structure in Thermomechanically Strengthened High-Nitrogen Steels, *Mater. Sci. Eng. A*, 2006, **438–440**, p 228–232
9. F. Xiao, B. Liao, G. Qiao, and S. Guan, Effect of Hot Deformation on Phase Transformation Kinetics of 86CrMoV7 Steel, *Mater. Charac.*, 2005, **57**, p 306–313
10. A.C. Kneissl, C.I. Garcia, and A.J. DeArdo, Characterization of Precipitates in HSLA Steel. *HSLA Steels: Processing, Properties and Applications*. The Minerals, Metals and Materials Society, USA, 1992, p 99–105
11. Y. Degang, *Theory of Microstructure and Strength of Steel*. Shanghai Sci Technol Press, Shanghai, 1983, p 100–108